

# Analytic model for galaxy and dark matter clustering

Uroš Seljak

*Department of Physics, Jadwin Hall, Princeton University, Princeton, NJ 08544*

(January 2000)

We investigate an analytic model to compute nonlinear power spectrum of dark matter, galaxies and their cross-correlation. The model is based on Press-Schechter halos, which cluster and have realistic dark matter profiles. The total power spectrum is a sum of two contributions, one from correlations between the halos and one from correlations within the same halo. We show that such a model can give dark matter power spectra which match well with the results of N-body simulations, provided that concentration parameter decreases with the halo mass.

Galaxy power spectrum differs from dark matter power spectrum because pair weighted number of galaxies does not scale with the halo mass and because most halos harbor a central galaxy. If the pair weighted number of galaxies increases less rapidly than the halo mass, as predicted by theoretical models and observed in clusters, then the resulting power spectrum becomes a power law with the slope closer to the observed over several orders of magnitude in scale. Such a model also predicts later onset of nonlinear clustering compared to the dark matter, which is needed to reconcile the CDM models with the data. Generic prediction of this model is that bias is scale dependent and nonmonotonic. This is particularly important for red or elliptical galaxies, which are preferentially found in larger mass halos and for which bias in power spectrum may be scale dependent even on large scales.

Our predictions for galaxy-dark matter correlations, which can be observed through the galaxy-galaxy lensing, show that these cannot be interpreted simply as an average halo profile of a typical galaxy, because different halo masses dominate at different scales and because larger halos host more than one galaxy. We compute predictions for the cross-correlation coefficient as a function of scale and discuss the prospects of using cross-correlations in combination with galaxy clustering to determine the dark matter power spectrum.

## I. INTRODUCTION

Correlations in dark matter contain a wealth of information about cosmological parameters. Their power spectrum is sensitive to parameters such as matter density, Hubble constant, primordial power spectrum slope and amplitude, massive neutrinos, baryon density etc. Determining the linear power spectrum of dark matter is one of the main goals of modern cosmology. There are several complications that prevent us at present from reaching this goal. First, on small scales the linear power spectrum is modified by nonlinear evolution which enhances its amplitude over the linear spectrum. It is important to understand this process, so that one can predict the relation between the two. This is necessary both to reconstruct the linear spectrum from a measured nonlinear one and to verify whether there are other mechanisms besides gravity that modify the clustering of dark matter on small scales. Examples of such are baryonic feedback effects on dark matter [1] or nongravitational interactions between dark matter particles [2]. Second, it is difficult to observe correlations in dark matter directly. Direct tracers such as peculiar velocity flows or weak lensing still suffer from low statistics and poorly understood systematics. Instead it is much easier to observe correlations between galaxies [3] or correlations between galaxies and dark matter [4]. While these are related to the dark matter correlations, the relation may not be simple. The goal of this paper is to address both issues with a model that is simple enough to allow analytic calculations without the use of N-body simulations, yet sufficiently accurate to be useful for predicting galaxy and dark matter power spectrum.

Our approach to dark matter clustering is based on the Press & Schechter model [6]. In this picture at any given time all the matter in the universe is divided into virialized halos. These halos are correlated and have some internal density profile, which can be a function of halo mass. By specifying the halo mass function, their clustering strength and their halo profile we can determine the dark matter correlation function. The formalism for correlations inside halos has been developed by [7] and applied to power law halos [8]. We generalize this approach by including the correlations between halos and by using more realistic non-power law halo profiles whose shape may depend on the halo mass [9]. We show in this paper that such a generalized model can provide very good agreement with results of numerical simulations over a wide range of scales [10].

The central question in extracting dark matter power spectrum from that of the galaxies is how well galaxies trace dark matter, the issue of bias. This has been addressed theoretically both with hydrodynamic [11] and semi-analytic methods [12,13]. The fact that the galaxy correlation function is a power law over several decades in scale, while power spectra in CDM models do not show such behaviour, already indicates that the bias is scale dependent.

Moreover, galaxies come in different types and observational data show that they can be biased relative to one another [14]. In our modelling of galaxy correlations we introduce two new functions, the mean number and the mean pair weighted number of galaxies inside the halo as a function of the halo mass. The importance of these has recently been emphasized in the context of pairwise velocity measurements [15,16] and galaxy clustering [12]. These play a key role in understanding the relation between galaxy and dark matter clustering. We explore the predictions for different choices of these relations and compare them to the results of semi-analytic models.

Galaxy-dark matter correlations can provide additional information on the clustering of galaxies and dark matter and the relation between them. Such correlations have been observed through gravitational lensing effects, for example using galaxy-galaxy lensing or correlations between foreground and background populations [4]. Such measurements are often interpreted either in terms of an averaged density profile of a halo [5] or in terms of a constant bias model [18]. We discuss the applicability of these models and how they can be generalized to take into account effects such as broad range of halo masses and multiple galaxies inside halos.

## II. DARK MATTER POWER SPECTRUM

The halo model for power spectrum assumes all the matter is in a form of isolated halos with a well defined mass  $M$  and halo profile  $\rho(r, M)$ . The halo profile is defined to be an average over all halos of a given mass and does not necessarily assume all halos have the same profile. The mass is determined by the total mass within the virial radius  $r_v$ , defined to be the radius where the mean density within it is  $\delta_{\text{vir}}$  times the mean density of the universe. Throughout the paper we will use  $\Lambda$ CDM model with  $\Omega_m = 0.3$ ,  $\Omega_\Lambda = 0.7$ , normalized to  $\sigma_8 = 0.9$  today. For this model  $\delta_{\text{vir}} \sim 340$ , although we will also use  $\delta_{\text{vir}} \sim 200$  (the value for Einstein-de Sitter universe) for consistency with the results of some of the N-body simulations. The halo profile is spherically averaged and assumed to depend only on the mass of the halo. We will model the halo density profile in the form

$$\rho(r) = \frac{\rho_s}{(r/r_s)^{-\alpha}(1+r/r_s)^{3+\alpha}}. \quad (1)$$

This model assumes that the profile shape is universal in units of scale radius  $r_s$ , while its characteristic density  $\rho_s$  at  $r_s$  or concentration  $c = r_v/r_s$  may depend on the halo mass. The halo profile is assumed to go as  $r^{-3}$  in the outer parts and as  $r^\alpha$  in the inner parts, with the transition between the two at  $r_s$ . The outer slope is fixed by the results of N-body simulations which generally agree in this regime. An example of such a profile is  $\alpha = -1$  [9,19,20]. Other models have however been proposed with  $\alpha = -1.5$  [21,22] or even  $\alpha > -1$  [23]. In principle  $\alpha$  could also be a function of mass scale and may steepen towards smaller mass halos with  $\alpha \sim -1$  for cluster halos and  $\alpha \sim -1.5$  for galactic halos [24]. Similarly, concentration  $c$  may depend on the mass and different authors find somewhat different dependence [9,21,25]. We will explore how variations in the profile and concentration affect the power spectrum. Instead of  $r_s$  we use the concentration parameter  $c = r_v/r_s$  as a free parameter. Note that  $r_v$  is related to  $M$  via  $M = 4\pi/3r_v^3\delta_{\text{vir}}\bar{\rho}$ . Similarly we can eliminate  $\rho_s$  and describe the halo only in terms of its virial mass  $M$  and concentration  $c$ , because the integral over the halo density profile (equation 1) must equal the halo mass.

For a complete description we need the halo mass function  $dn/dM$ , describing the number density of halos as a function of mass. It can be written as

$$\frac{dn}{dM}dM = \frac{\bar{\rho}}{M}f(\nu)d\nu, \quad (2)$$

where  $\bar{\rho}$  is the mean matter density of the universe. We introduced function  $f(\nu)$ , which can be expressed in units in which it has a universal form independent of the power spectrum or redshift if written as a function of peak height

$$\nu = [\delta_c(z)/\sigma(M)]^2. \quad (3)$$

Here  $\delta_c$  is the value of a spherical overdensity at which it collapses at  $z$  ( $\delta_c = 1.68$  for Einstein-de Sitter model) and  $\sigma(M)$  is the rms fluctuation in spheres that contain on average mass  $M$  at initial time, extrapolated using linear theory to  $z$ . The form proposed by Press & Schechter (PS) [6] is  $\nu f(\nu) = (\nu/2\pi)^{1/2}e^{-\nu/2}$ . This has been shown to overpredict the halo abundance by a factor of 2 at intermediate masses below nonlinear mass scale  $M_*$  [26,27]. A modified version of this form that fits better the N-body simulations is given by Sheth & Tormen (ST) [27]

$$\nu f(\nu) = A(1 + \nu'^{-p})\nu'^{1/2}e^{-\nu'/2}, \quad (4)$$

where  $\nu' = a\nu$  with  $a = 0,707$  and  $p = 0.3$  as the best fitted values, which gives  $\nu f(\nu) \propto \nu^{0.2}$  for small  $\nu$ . PS expression corresponds to  $a = 1$ ,  $p = 0$  giving  $\nu f(\nu) \propto \nu^{0.5}$  for small  $\nu$ . The constant  $A$  is determined by mass conservation, requiring that the integral over the mass function times the mass gives the mean density

$$\frac{1}{\bar{\rho}} \int \frac{dn}{dM} M dM = \int f(\nu) d\nu = 1. \quad (5)$$

Note that we can still apply this equation even if some dark matter is not bound to any halo. In this case the mass function has a nonvanishing contribution in the limit  $M \rightarrow 0$ .

The correlation function consists of two terms. On large scales the halos are correlated with each other. We assume the halo-halo correlation function follows the linear correlation function. Its amplitude depends on the bias for each halo. Halos more massive than the nonlinear mass scale  $M_*$  are more strongly clustered than the matter, while those with masses below  $M_*$  are less strongly clustered than the matter. A simple halo biasing scheme has been given by [28,29] and generalized to the ST mass function by [27]

$$b(\nu) = 1 + \frac{\nu - 1}{\delta_c} + \frac{2p}{\delta_c(1 + \nu^p)}. \quad (6)$$

Since halos are not pointlike we need to convolve the halo-halo correlation function with the halo profiles of both halos to obtain the dark matter correlation function. The expressions simplify significantly in Fourier space, where convolution becomes a multiplication with the Fourier transform of the halo profile

$$\tilde{\rho}(k, M) = \int 4\pi r^2 dr \rho(r, M) \frac{\sin(kr)}{kr}. \quad (7)$$

Note that this is normalized so that  $\tilde{\rho}(0, M) = M$ . It is convenient to renormalize it to unity by introducing a new variable  $y(k, M) = \tilde{\rho}(k, M)/M$ , so that  $y(0, M) = 1$  and  $y(k > 0, M) < 1$ . The mass of the halo rapidly increases as  $r^{3-\alpha}$  up to  $r = r_s$ , but increases only logarithmically between  $r_s$  and  $r_v$  if the outer profile is  $\rho(r) \propto r^{-3}$ . The dominant contribution to the mass therefore comes from radii around  $r_s$ . For  $kr_s \ll 1$  we have  $y \approx 1$ . At  $kr_s \sim 1$  there is a transition and  $y$  begins to decrease with  $k$ , so that for  $kr_s \gg 1$  we have  $y(k, M) \propto (kr_s)^{-(3+\alpha)}$ .

Because the expressions simplify significantly in Fourier space we will in the following only describe the power spectrum analysis. The halo-halo term is given by the integral over their mass function with the appropriate bias and the halo profile transform,

$$P_{\text{dm}}^{hh}(k) = P_{\text{lin}}(k) \left[ \int f(\nu) d\nu b(\nu) y[k, M(\nu)] \right]^2, \quad (8)$$

where  $P_{\text{lin}}(k)$  is the linear power spectrum and  $M$  is related to  $\nu$  via equation 3 using the relation between  $\sigma^2(M) = 4\pi \int P_{\text{lin}}(k) W_R(k) k^2 dk$  and  $M = 4\pi R^3 \bar{\rho}/3$ , where  $W_R(k)$  is the Fourier transform of the top hat window with radius  $R$ . This gives  $M \propto \nu^{3/(n+3)}$ , where  $n$  is the slope of the linear power spectrum at scale  $k \sim R^{-1}$ . We can also define the nonlinear mass scale  $M_*$  where  $\nu = 1$ . Note that on galaxy and smaller scales  $n < -2$  and the relation between  $M$  and  $\nu$  is very steep,  $M \propto \nu^\gamma$  with  $\gamma > 3$ . The requirement that on large scales ( $k \rightarrow 0, y \sim 1$ ) the power spectrum reduces to the linear power spectrum imposes a nontrivial constraint on the bias distribution,

$$\int f(\nu) d\nu b(\nu) = 1. \quad (9)$$

This implies that if halos are biased ( $b > 1$ ) for  $M > M_*$  at least some of the halos with  $M < M_*$  must be antibiased ( $b < 1$ ) to satisfy this constraint. Most of the bias descriptions in the literature satisfy this constraint to within a few percent. The halo-halo term follows the linear power spectrum on large scales and drops below it on scales where finite extent of the halos become important (ie where  $y(k, M) < 1$ ). This term is shown in figure 1 and as expected is dominant on large scales.

In addition to the halo-halo correlation term there are also correlations between dark matter particles within the same halos. These are expected to dominate on small scales. We denote this the Poisson term, which is given by

$$P_{\text{dm}}^P(k) = \frac{1}{(2\pi)^3} \int f(\nu) d\nu \frac{M(\nu)}{\bar{\rho}} |y[k, M(\nu)]|^2, \quad (10)$$

The main difference between this term and the halo-halo term in equation 8 is that we have an additional mass weighting  $M/\bar{\rho}$ . This makes the dominant contribution to this term to come from the higher mass halos relative to the halo-halo term. On large scales ( $k \rightarrow 0, y \sim 1$ ) the Poisson term is independent of  $k$  and behaves as white noise. It increases with  $k$  more rapidly than the halo-halo term, which scales as the linear power spectrum (figure 1). The Poisson term declines below the white noise on small scales where the effects of the halo profile become important.

The total power spectrum is the sum of the two contributions,

$$P_{\text{dm}}(k) = P_{\text{dm}}^{hh}(k) + P_{\text{dm}}^P(k). \quad (11)$$

To complete the calculation we need to model the dependence of  $c$  on  $M$ . We will parametrize it as

$$c = c_0(M/M_*)^\beta. \quad (12)$$

Typical values for  $c_0$  are around 10 at the nonlinear mass scale for  $\alpha = -1$  profile [9,25] and about a third lower for  $\alpha = -1.5$  profile [21]. Numerical studies also show that the concentration decreases slowly with the halo mass, making  $\beta$  negative.

Figure 1 shows the individual contributions and the sum in comparison to the linear power spectrum and the nonlinear prediction from [31] (PD). In top of the figure we used  $\alpha = -1.5$  and  $c(M) = 6(M/M_*)^{-0.15}$ . The latter fits the concentration mass dependence given in [21]. Note that for consistency with [21] we use  $\delta_{\text{vir}} = 200$  in this case as opposed to  $\delta_{\text{vir}} = 340$ . In bottom of the figure we used the ST mass function and  $\alpha = -1$  with  $c(M) = 10(M/M_*)^{-0.2}$ , which is somewhat steeper than numerical studies predict [25] as discussed below. The agreement in both cases is quite remarkable given the simple nature of the model. It correctly predicts the transition between the linear and nonlinear power spectrum, as well as reproduces well the slope at higher values of  $k$ . This shows that given a suitable choice of  $c(M)$  both models can reproduce the nonlinear power spectrum. Conversely, the slope of the power spectrum at high  $k$  is not directly determined by the inner slope of dark matter profiles, at least if the inner profiles are shallower than  $\alpha = -1.5$ .

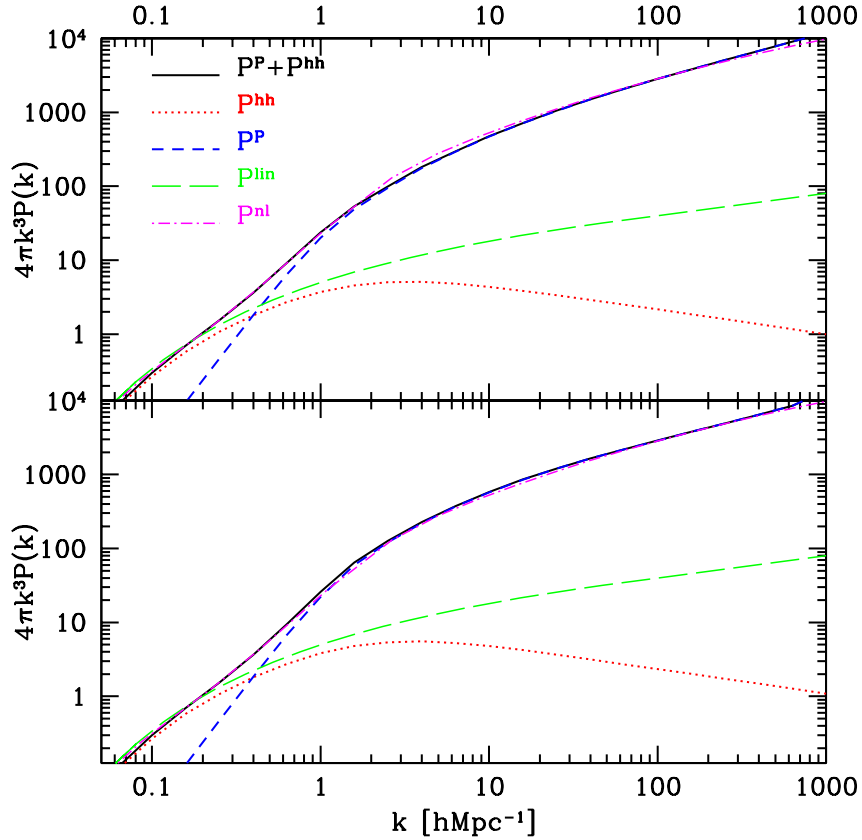


FIG. 1. Comparison between the power spectrum predicted with our model and the PD nonlinear power spectrum for  $\Lambda$ CDM model. Also shown are the linear power spectrum and the two individual contributions,  $P^P$  and  $P^{hh}$ . Top is the  $\alpha = -1.5$  profile, bottom is  $\alpha = -1$ . Other parameters are given in the text.

In the case of  $\alpha = -1$  profile the best fitted value for  $c_0 = 10$  agrees well with [25,9], while  $\beta \sim -0.2$  is somewhat lower than  $\beta = -0.07$  [9] and  $\beta = -0.13$  [25]. If one adopts such shallow dependence of  $c(M)$  with  $\beta \sim -0.1$  then for  $k > 10h\text{Mpc}^{-1}$  the predictions of the model are systematically below the PD model. Before concluding that this is caused by the galactic halos not being sufficiently compact we must investigate the possibility that the mass function is underestimated at small masses. Replacing ST with PS does not significantly affect the results. However, both PS and ST assume that each mass element belongs to only one halo, counting only the isolated halos. This

is certainly a valid description on large scales, where the total halo mass determines the white noise amplitude of the power spectrum. On small scales the clumpiness caused by subhalos within the halos may become important. Recent numerical simulations have in fact shown that most of the small halos that merge into larger ones are not immediately destroyed, but stay around for some time until they are finally merged on the dynamical friction time scale [30,21,23]. In such a case a given mass particle can be part of more than one halo at any given time. Because on very small scales the correlation function is dominated by the small halos it may make a difference whether the mass is smoothly distributed within the halos or some fraction of it is in the subhalos. However, the contribution to the total mass of the halo coming from the subhalos is below 10% [23,20]. Recently, the mass function for subhalos from high resolution simulations was determined and it was shown that it is an order of magnitude below the one for isolated halos [32]. One may conclude therefore that subhalos do not affect the mass function significantly and cannot resurrect  $\beta > -0.13$ ,  $\alpha = -1$  model.

Steepening the halo profile or changing concentration can both increase the power spectrum to agree better with N-body simulations (figure 1). This is because to increase the power on small scales one has to increase the amount of mass contained within a given radius. This can be achieved either by making the inner profile steeper than  $\alpha = -1$  or making the concentration parameter larger towards the smaller mass halos. The change in the slope would support the results in [21,22], where the universal profile has the inner slope close to  $\alpha \sim -1.5$ , or in [24], where the profile is not universal and steepens as the halo mass is decreased, so that the inner slope changes from  $\alpha \sim -1$  on the cluster scales to  $\alpha \sim -1.5$  on the galactic scales. If the inner slope of the halo profile is  $\alpha \sim -1$  the concentration has a stronger mass dependence than in [9,25], although the discrepancy is not large. As shown in figure 1 both models can fit the nonlinear power spectrum on small scales remarkably well.

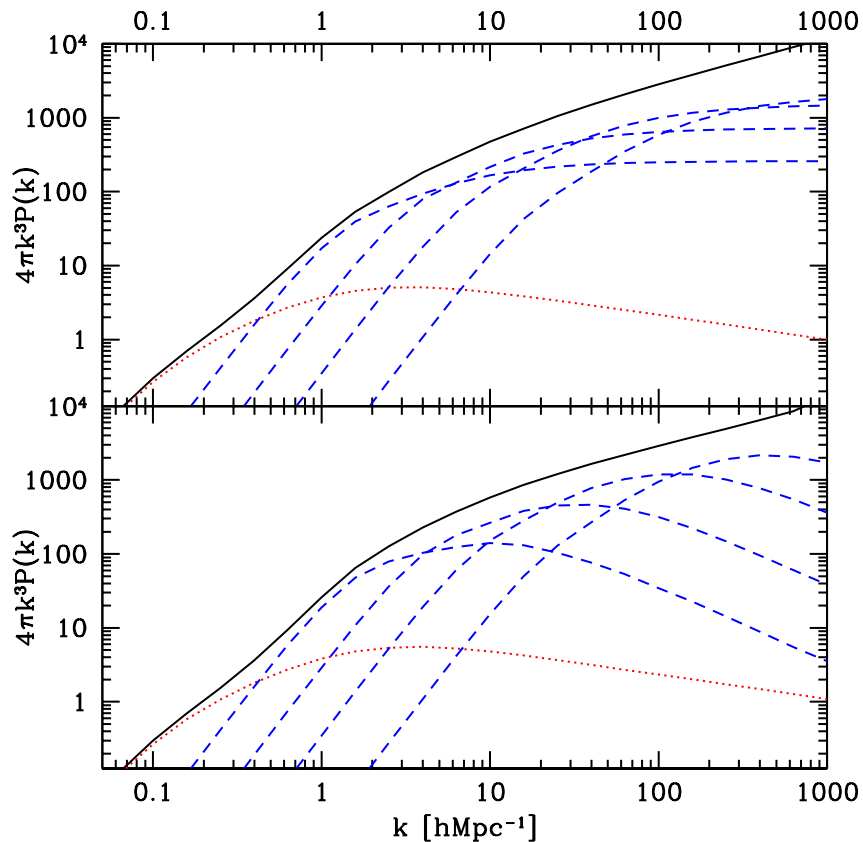


FIG. 2. Contribution to the  $P^P(k)$  from different halo mass intervals for the two models in figure 1. Short dashed lines from left to right are  $M > 10^{14}h^{-1}M_\odot$ ,  $10^{14}h^{-1}M_\odot > M > 10^{13}h^{-1}M_\odot$ ,  $10^{13}h^{-1}M_\odot > M > 10^{12}h^{-1}M_\odot$  and  $10^{12}h^{-1}M_\odot > M > 10^{11}h^{-1}M_\odot$ . Solid line is the total  $P(k)$ , dotted the correlated term  $P^{hh}(k)$ .

Further insight into the relation between the halos and the dark matter power spectrum can be obtained by investigating the contribution to the power spectrum from different mass intervals. This is shown in figure 2 for the Poisson term, using the two models from figure 1. On large scales the Poisson term is dominated by very massive clusters with  $M > 10^{14}h^{-1}M_\odot$ . These halos dominate the nonlinear clustering on scales around and below

$k < 1h\text{Mpc}^{-1}$ . On smaller scales the contribution from large clusters is suppressed because  $y(k, M)$  begins to decrease from unity at  $k \sim r_c^{-1} \propto c(M)M^{-1/3} \propto M^{-0.5}$ . This occurs at lower  $k$  for the higher mass halos. As a result around  $k \sim 10h\text{Mpc}^{-1}$  the halos with  $10^{14}h^{-1}M_\odot > M > 10^{13}h^{-1}M_\odot$  dominate, while around  $k \sim 100h\text{Mpc}^{-1}$  the halos with  $10^{13}h^{-1}M_\odot > M > 10^{12}h^{-1}M_\odot$  dominate. Note again that the inner slope plays a subdominant role in determining the amplitude of the power spectrum. Even if for a steeper slope the power spectrum from a given mass interval is decreasing less rapidly (for example for  $\alpha = -1.5$  it is asymptotically flat as opposed to decreasing as  $k^{-1}$  for  $\alpha = -1$ ), when this becomes important the smaller mass halos have already taken over as a dominant contribution to the power spectrum. The nonlinear power spectrum therefore does not reflect the inner slope of the halo profile, but rather the halo mass function and the radius at which the mass enclosed within this radius begins to deviate significantly from the total halo mass. In both models the halos with  $M > 10^{11}h^{-1}M_\odot$  dominate the power spectrum for  $k < 100h\text{Mpc}^{-1}$ . Any modifications in the linear power spectrum on mass scales below  $M \sim 10^{11}h^{-1}M_\odot$  [33] would therefore show up in the dark matter correlation function only on kiloparsec scales and below.

It is interesting to explore in more detail the quasi-linear regime, where  $P^P(k) \sim \text{const}$ . This approximation is valid up to  $4\pi k^3 P(k) \sim 10$  or  $k \sim 1h\text{Mpc}^{-1}$ . On scales larger than these the power spectrum can be approximated as a sum of a linear power spectrum and a constant term, whose amplitude is given as an integral over the mass function (equation 10 with  $y = 1$ ). From figure 2 one can see that the amplitude of this integral is dominated by the massive halos,  $M > 10^{14}h^{-1}M_\odot$ . It is important to emphasize that this amplitude depends only on the integral over the power spectrum and not on the details of the power spectrum itself. Even if there are sharp features in the linear power spectrum, such as for example baryonic wiggles [34], these would not show up as features in the quasi-linear power spectrum. Instead, they would be integrated over into a single number, corresponding to the mass weighted integral over the mass function (equation 10). This argument is in agreement with the results of N-body simulations [35] which indeed show that any baryonic features are erased in the nonlinear regime. This suggests that while the PD model breaks down for such spectra, our model could also be applied in such a case. This also applies to the spectra with truncated power on small scales [36]. We plan to investigate this further in the future.

### III. GALAXY POWER SPECTRUM

We now apply the above developed model to the galaxies. We assume all the galaxies form in halos, which is a reasonable assumption given that only very dense environments which have undergone nonlinear collapse allow the gas to cool and to form stars. The key new parameters we introduce are the mean number of galaxies per halo as a function of halo mass,  $\langle N \rangle(M)$ , and the mean pair weighted number of galaxies per halo,  $\langle N(N-1) \rangle^{1/2}(M)$ . Just as in the case of dark matter these functions are well defined even if the assumption that the statistical properties of galaxy population depend only on the halo mass and not on its environment is not satisfied [11], as long as the averaging is performed over all possible environments. The resulting power spectrum on small scales where the Poisson term dominates is independent of this assumption. On large scales where correlations between the halos are important violation of this assumption may lead to a change in the strength of the halo-halo term.

We furthermore assume that there each halo has a galaxy at its center, while the rest of the galaxies in the halos are distributed in the same way as the dark matter, so  $y(k, M)$  remains unchanged. This is only the simplest model and one could easily generalize it to profiles that differ from the dark matter. Any such complications are important on small scales, while on large scales ( $k < 1h\text{Mpc}^{-1}$ ) all that is relevant is the total number of galaxies inside the halo. The normalization equation 9 becomes

$$\int \frac{\langle N \rangle}{M} f(\nu) d\nu = \frac{\bar{n}}{\bar{\rho}}, \quad (13)$$

where  $\bar{n}$  is the mean density of galaxies in the sample.

The halo-halo correlation term is given by

$$P_{\text{gg}}^{hh}(k) = P_{\text{lin}}(k) \left[ \frac{\bar{\rho}}{\bar{n}} \int f(\nu) d\nu \frac{\langle N \rangle}{M} b(\nu) y(k, M) \right]^2. \quad (14)$$

This should be modified somewhat because the central galaxy does not contribute a  $y(k, M)$  term, but this is only important on small scales where the halo-halo term is negligible. On large scales where  $y \sim 1$  this term gives the constant bias model

$$P_{\text{gg}}^{hh}(k) = \langle b \rangle^2 P_{\text{lin}}(k), \quad (15)$$

where the mean galaxy bias  $\langle b \rangle$  is given by

$$\langle b \rangle = \frac{\bar{\rho}}{\bar{n}} \int f(\nu) d\nu \frac{\langle N \rangle}{M} b(\nu). \quad (16)$$

The Poisson term is given by

$$P_{\text{dm}}^P(k) = \frac{\bar{\rho}^2}{(2\pi)^3 \bar{n}^2} \int \frac{M}{\bar{\rho}} f(\nu) d\nu \frac{\langle N(N-1) \rangle}{M^2} |y(k, M)|^P. \quad (17)$$

We use the approximation with  $p = 2$  if  $\langle N(N-1) \rangle > 1$ , because in the limit the number of pairs is large it is dominated by the halo galaxies, and  $p = 1$  if  $\langle N(N-1) \rangle < 1$ , because in the opposite limit the number of pairs in this case is dominated by the central galaxy paired with a halo galaxy. Following the usual convention [37] we use  $\langle N(N-1) \rangle$  instead of  $\langle N^2 \rangle$ , since we subtract out the shot noise term arising from the discrete nature of galaxies (such a term does not depend on the halo profile  $y(k, M)$ ). Comparing equations 8 and 10 with equations 14 and 17 we see that there is no difference between the two only if  $\langle N \rangle / M$  and  $\langle N(N-1) \rangle^{1/2} / M$  are independent of  $M$ , there are many galaxies per halo and the galaxies are distributed as the dark matter within the halo. For such conditions the power spectrum of galaxies is identical to the power spectrum of dark matter.

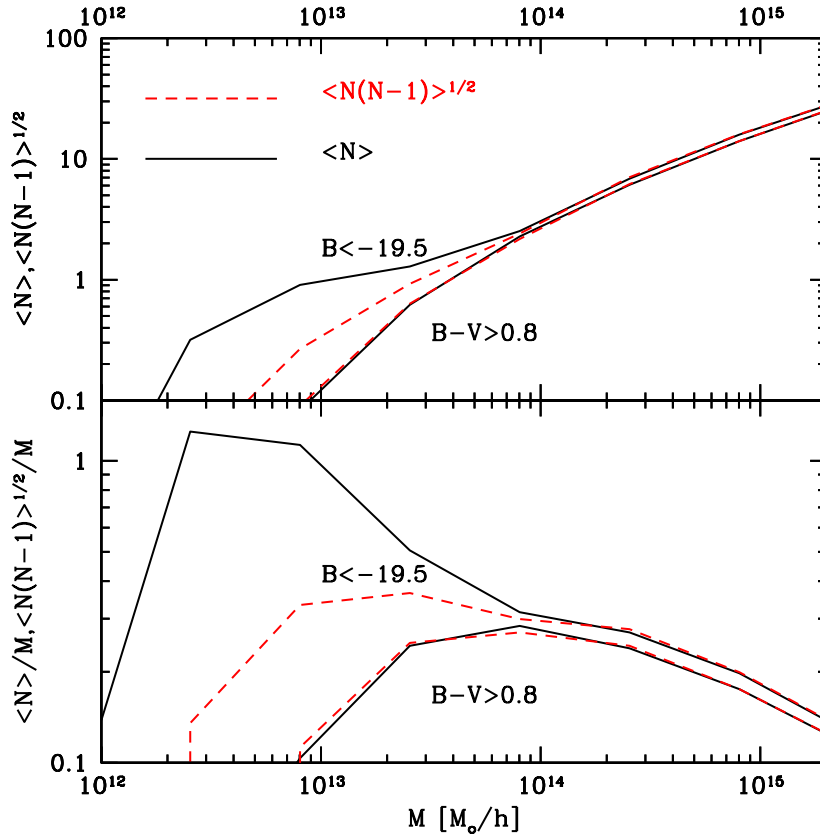


FIG. 3. Top figure shows  $\langle N(N-1) \rangle^{1/2}$  and  $\langle N \rangle$  versus  $M$  for galaxies selected by absolute magnitude  $M_B < -19.5$  (upper curves) and color  $M_B < -19.5$ ,  $M_B - M_V > 0.8$  (lower curves) from semi-analytic models. Bottom figure shows the same functions divided by  $Mh/10^{13} M_\odot$ .

To test the model above we use semi-analytic models of galaxy formation developed in [13]. These models use N-body simulations to identify the halos and their progenitors. Gas is assumed to follow dark matter initially so that it heats up during the collapse to the virial temperature of the halo. Because of the high density it can efficiently cool and subsequently concentrate at the center of the halo. Stars are formed from this cold gas on the dynamical time scale. The parametrized star formation efficiency and the stellar population synthesis models are used to assign magnitudes in different color bands to the formed galaxies. The small halos with galaxies in them subsequently merge into larger halos and exist as individual galaxies until they merge with the central galaxy on the dynamical friction time scale. The output of these models is a catalog of halos and their masses. For each halo the output consists of a list of galaxies, their positions and luminosities in different bands. From such a catalog one can reconstruct

the 3-d distribution of galaxies and dark matter, as well as  $\langle N \rangle$  and  $\langle N(N-1) \rangle^{1/2}$  averaged over a given range of halo masses for any desired galaxy selection criterion. The goal of our comparison is to compare the galaxy power spectrum predicted from our model using  $\langle N \rangle(M)$  and  $\langle N(N-1) \rangle^{1/2}(M)$  from semi-analytic models to the galaxy power spectrum obtained directly from these models. This is a meaningful comparison even if semi-analytic models do not correctly describe the nature. If we determine that the model contains all the necessary ingredients to predict the galaxy correlations we can then try to obtain these ingredients by other means, either through direct observations or better modelling. This can also be applied in the other direction: from observations of galaxy power spectrum (and galaxy-dark matter power spectrum discussed in the next section) we can determine the ingredients of our model, which must be satisfied by any theoretical galaxy formation model.

A generic outcome of theoretical models such as these is that the amount of cold gas that can be transformed to stars increases as a function of the mass slower than the halo mass itself, because larger halos are hotter and the gas takes longer to cool [11,13,12]. In such models one would expect  $\langle N \rangle/M$  to decline with  $M$ . This is shown in figure 3 where  $\langle N \rangle$  and  $\langle N(N-1) \rangle^{1/2}$  is plotted versus  $M$  for galaxies selected only on the basis on absolute magnitude ( $M_B < -19.5$ ). Both functions have similar dependence for  $M > 10^{14} h^{-1} M_\odot$ . When the number of galaxies per halo begins to drop below unity the two functions begin to deviate from one another and  $\langle N(N-1) \rangle^{1/2}$  drops below  $\langle N \rangle$ . This is because only the halos with two or more galaxies contribute to  $\langle N(N-1) \rangle^{1/2}$ , while single galaxy halos also contribute to  $\langle N \rangle$ . However, both functions increase less rapidly than the mass for  $M > 10^{13} h^{-1} M_\odot$ .

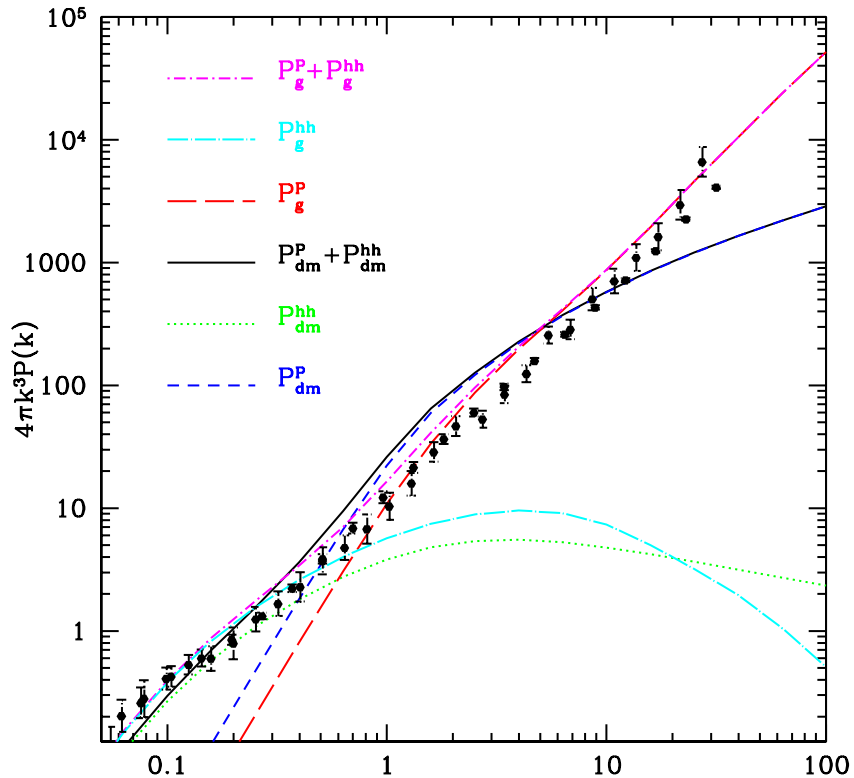


FIG. 4. Comparison between galaxy and dark matter power spectrum predictions for galaxies selected by absolute magnitude  $M_B < -19.5$  as in figure 3. Poisson, halo-halo and combined terms are shown for the two spectra. Also shown is the measured power spectrum of galaxies. Note that at low  $k$  the Poisson term for the galaxies is lower than that for the dark matter and this delays the onset of nonlinear clustering in galaxies.

Using  $\langle N(N-1) \rangle^{1/2}/M$  and  $\langle N \rangle/M$  for  $M_B < -19.5$  from figure 3 in equations 13-17 we obtain the galaxy power spectrum shown in figure 4. We only show results for  $\alpha = -1$  model, but the  $\alpha = -1.5$  model gives essentially identical results. Also shown is the dark matter power spectrum and its two contributions, as well as the measured APM and scaled IRAS galaxy power spectrum compiled in [3]. First thing to note is the good agreement between our analytical model and the simulations. The agreement is significantly better for this model than for the model where there is no central galaxy, which would give a stronger decline in power on small scales. The galaxy power spectrum

is almost a perfect power law over several decades in scale, in agreement with observations and in contrast to the dark matter power spectrum, whose slope gradually decreases with  $k$ . The slope of the galaxy power spectrum is in agreement with the observed slope  $k^3 P(k) \propto k^{1.8}$  and this slope persists in the analytic model down to kpc scales.

It is useful to introduce bias  $b(k)$ , defined as the square root of the ratio between galaxy and dark matter power spectrum,

$$b(k) = [P_{\text{gg}}(k)/P_{\text{dm, dm}}(k)]^{1/2}. \quad (18)$$

The bias  $b(k)$  is approximately constant and close to unity on large scales, decreases and becomes less than unity between  $0.3\text{hMpc}^{-1} < k < 6\text{hMpc}^{-1}$  and then increases for large  $k$ . The bias is therefore scale dependent and nonmonotonic, both of which as shown below are generic predictions of this model. On very large scales the power spectrum is dominated by the correlations between the halos and the internal structure of halos can be neglected. This gives the constant bias on large scales, which for the galaxy type considered here is close to unity. On smaller scales the halo Poisson term becomes important both for galaxies and dark matter. However, if  $\langle N(N-1) \rangle^{1/2}/M \propto M^\psi$  with  $\psi < 0$  the Poisson term for galaxies is lower than the Poisson term for dark matter in the limit  $y(k, M) = 1$ . This is because the halo Poisson term is larger if halos are rarer. If  $\psi < 0$  the dominant contribution in galaxy power spectrum is shifted to lower mass halos, which are more abundant and this reduces the Poisson term relative to dark matter. Another important factor that reduces the galaxy Poisson term is that  $\langle N \rangle$  exceeds  $\langle N(N-1) \rangle^{1/2}$  below  $M \sim 10^{14} h^{-1} M_\odot$ .  $\langle N \rangle(M)$  determines the mean density of galaxies  $\bar{n}$  in equation 13. This suppresses the Poisson term in equation 17 even if  $\psi = 0$ . Suppression of the galaxy Poisson term relative to the dark matter delays the onset of nonlinear power in the galaxy power spectrum relative to the dark matter, which is clearly seen in figure 4. It gives a natural explanation for the position of the inflection point in the observed galaxy power spectrum without the need to introduce phenomenological double power law spectra [3]. While our model is already in a good agreement with the data an even better fit would be achieved with a somewhat smaller Poisson term, which would require  $\psi$  to be even lower or  $\langle N \rangle$  to exceed  $\langle N(N-1) \rangle^{1/2}$  even more. This would further delay the onset of the nonlinear clustering.

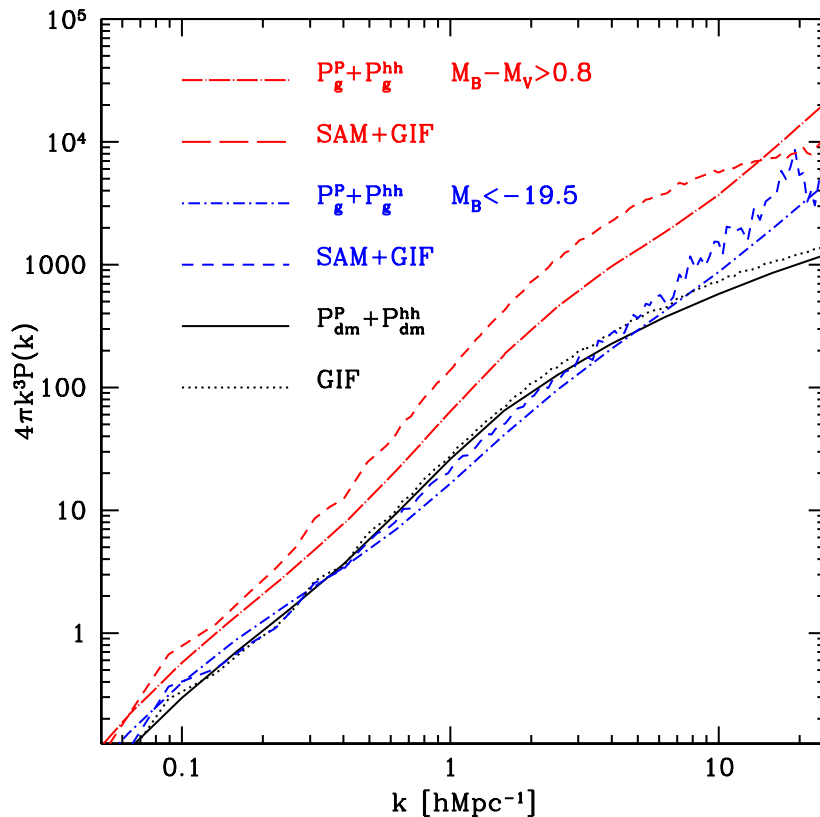


FIG. 5. Comparison between galaxy and dark matter power spectrum predicted by our model and the results of N-body simulations and semi-analytic models. Predictions for galaxies selected by absolute magnitude  $M_B < -19.5$  and  $M_B - M_V > 0.8$  are shown.

On even smaller scales the halo profile  $y(k, M)$  becomes important, since it begins to decrease from unity at a scale that corresponds to a typical size of the halo, which is smaller for the lower mass halos. Since the galaxy power spectrum is weighted towards lower mass halos relative to dark matter the term  $y(k, M)$  begins to be important in suppressing the Poisson term at a smaller scale. In addition, if each halo hosts a central galaxy then switching to  $p = 1$  for small halos also makes the suppression by the halo profile less important. Smaller suppression of the galaxy power spectrum relative to the dark matter results in an increase of bias with  $k$ . This argues that the decrease of  $b(k)$  on intermediate scales and the increase on small scales are generic predictions. The overall result of this is an approximate power law of the galaxy power spectrum over several decades. Such a power law arises quite generically in a CDM family of models where  $\psi < 0$  (or  $\langle N \rangle > \langle N(N - 1) \rangle^{1/2}$ ) and where each halo hosts a central galaxy. We note that the latter is required to preserve the power law behaviour to very small scales. A model where  $p = 2$  for all halo masses turns below the power law in the power spectrum at  $k > 50h\text{Mpc}^{-1}$ , similar to the dark matter.

The conclusion above that the bias first declines with  $k$  and then rises again applies to a normal galaxy population. If one selects red galaxies on the basis of color or ellipticals on the basis of morphology then one may expect a different bias dependence, since red or elliptical galaxies are preferentially found in more massive halos, such as groups and clusters. Figure 3 shows that the galaxies selected by  $M_B - M_V > 0.8$  and  $M_B < -19.5$  are dominant in halos with  $M > 10^{14}h^{-1}M_\odot$ , while their relative fraction declines rapidly below that. The dependence of  $\langle N(N - 1) \rangle^{1/2}$  with  $M$  is much steeper in this case so that  $\psi > 0$  for  $M < 10^{14}h^{-1}M_\odot$ . In addition  $\langle N \rangle \sim \langle N(N - 1) \rangle^{1/2}$  across the entire range of halo masses, a consequence of the fact that most of the red galaxies are not central galaxies, which in these models show recent star formation and are therefore not red.

Figure 5 shows the comparison between analytic predictions and results from semi-analytic models [13]. We use mass dependence from figure 3 in equations 13-17 for both  $M_B < -19.5$  and  $M_B - M_V > 0.8$  galaxy selection. Also shown are the dark matter power spectrum from the model and from the GIF simulations [38] which were used for semi-analytic models. Qualitatively the agreement is excellent, specially for dark matter and  $M_B < -19.5$  galaxies, while for red galaxies semi-analytic models predict a somewhat higher amplitude. Part of the disagreement is caused simply by dark matter spectrum not being in agreement with PD (our models are chosen so that they agree with PD) [38]. We do not show small scales ( $k > 20h\text{Mpc}^{-1}$ ) where limited resolution of N-body simulations prevents a meaningful comparison. The remaining discrepancy for red galaxies between  $0.5h\text{Mpc}^{-1} < k < 20h\text{Mpc}^{-1}$  can only be explained by them not tracing exactly dark matter distribution in halos with  $M > 10^{13}h^{-1}M_\odot$ . The red galaxies must be more centrally concentrated than dark matter in semi-analytic models in order that their power spectrum has a higher amplitude than predicted from our model. This is in agreement with direct analysis of galaxy distribution inside halos using the same simulations [39], where it was found that red galaxies in  $\Lambda\text{CDM}$  model tend to be more centrally concentrated than dark matter. Galaxies that form first end up more towards the center of the cluster because the violent relaxation during the merging is incomplete.

In the case of the red galaxies the bias starts with a value larger than unity on large scales. This is because most of the red galaxies are in clusters which are biased relative to the dark matter following equation 6. Bias first rises with  $k$  and then declines. This is just the opposite from the scale dependence of the normal galaxies and is a consequence of  $\psi > 0$  for  $M < 10^{14}h^{-1}M_\odot$  and  $\langle N \rangle \sim \langle N(N - 1) \rangle^{1/2}$ . This gives rise to the Poisson term larger for the galaxies than for the dark matter on large scales. This conclusion is again independent of the distribution of the galaxies inside the halos. This is confirmed in figure 5 where on large scales our model agrees very well with the semi-analytic predictions. Because the galaxies are preferentially in larger halos relative to the dark matter  $y(k, M)$  suppression is more important and the bias declines on smaller scales. This is seen in the power spectrum from the simulations. In our model it begins to rise again on even smaller scales because  $p$  switches to unity for  $M < 10^{14}h^{-1}M_\odot$ , resulting in a smaller suppression by the halo profile. This effect is not seen in the simulations, presumably because of their limited resolution.

It is important to note that bias may never be really constant even on scales above  $100h^{-1}\text{Mpc}$ . For the red sample it changes by 30% between  $k = 0.01h\text{Mpc}^{-1}$  and  $k = 0.1h\text{Mpc}^{-1}$ . This is because the Poisson term does not become much smaller than the halo-halo term even on very large scales, a consequence of the fact that the slope of  $P_{\text{lin}}(k)$  and thus the halo-halo term itself becomes flat and even positive on very large scales (approaching  $n \sim 1$  on very large scales). Since even at the turnover of the power spectrum (where  $n \sim 0$ ) the Poisson term for the red galaxies is of the order of 20% of the halo-halo term the bias does not become constant and begins to increase again on scales larger than the scale of the turnover. In fact on very large scales ( $k < 10^{-3}h\text{Mpc}^{-1}$ ) the red galaxy power spectrum becomes white noise, although these scales are already approaching the size of the visible universe. It should be noted that this description is valid on large scales only for galaxies which do not obey mass and momentum conservation. For the dark matter mass and momentum conservation require that the Poisson term vanishes on large scales and any spectrum generated by a local process should decrease faster than  $P(k) \propto k^4$  as  $k \rightarrow 0$  [40]. Galaxies do not obey mass and momentum conservation and can have the Poisson contribution, so the qualitative scale dependence of bias remains as predicted above.

We have concentrated on the power spectrum above because it is the quantity that can be most directly compared to the theoretical predictions. The same analysis could however be applied to the correlation function as well. The power law dependence of the power spectrum would also result in a power law correlation function, so the conclusions would remain unchanged. The main difference in the real space is that the Poisson term is localized to scales smaller than the typical halo scale and vanishes on scales above that. In this case bias would be scale dependent up to this typical scale (of order few Mpc), but would become scale independent on scales above that. There is no need to model the Poisson term on large scales at all. In this sense the real space correlation function offers some advantages over the power spectrum, where one must attempt to remove the Poisson term in the power spectrum by modelling it as a constant term on large scales.

Our predictions agree with the results of semi-analytic models, indicating that the here proposed model is sufficient to extract the key ingredients to model the galaxy clustering. This means one does not need to rely on N-body simulations as long as the ingredients of the model are specified. If one can extract  $\langle N \rangle$ ,  $\langle N(N-1) \rangle^{1/2}(M)$  and  $y(k, M)$  directly from the data one can sidestep the theoretical modelling of this relation and predict the galaxy power spectrum directly [41]. It is in principle possible to obtain such information at least for the massive halos by combining dynamical information on galaxy groups and clusters, such as X-ray temperature, velocity dispersion or weak lensing mass, with the number of galaxies in these clusters. Existing data such as CNOC survey [42] indeed find that  $\langle N \rangle/M$  for galaxies with  $M_K < -18.5$  is systematically lower in massive clusters with  $\sigma > 1000$  km/s than in poorer clusters. The current data are sparse, but new large surveys such as SDSS and 2dF will enable one to extract such information with a much better statistics. This could allow one to determine within our model the dark matter power spectrum from the galaxy power spectrum directly.

Another direction to obtain  $\langle N \rangle/M$  is to require consistency with other measurements that combine dynamical and galaxy information. Galaxy-dark matter correlations discussed in the next section are one possibility. Another are pairwise velocity dispersion measurements. If  $\langle N \rangle/M$  declines with  $M$  then the pairwise velocity dispersion for the galaxies will be lower than for the dark matter [15,16]. This is because there will be more pairs of galaxies in smaller halos relative to the dark matter. Smaller halos have smaller velocity dispersions and smaller relative velocities between the particles. This can explain the lower amplitude of pairwise velocity dispersion in the LCRS data compared to the N-body simulations [15]. The required value of  $\psi \sim -0.1$  has indeed the same sign as required to reproduce the delayed onset of nonlinear clustering and the power law in galaxy power spectrum. It would be interesting to see whether a single set of functions  $\langle N \rangle(M)$ ,  $\langle N(N-1) \rangle^{1/2}(M)$  can provide a unified description to both galaxy clustering and pairwise velocities within the CDM models.

#### IV. DARK MATTER-GALAXY CROSS-CORRELATION

Dark matter-galaxy cross-correlations are measured whenever a galaxy is cross-correlated with a tracer of the dark matter. Examples of this are galaxy-galaxy lensing [17], where one is measuring correlation between galaxies and cosmic shear, and correlations between foreground and background galaxies or quasars [4], where correlations (or anti-correlations) are induced by magnification bias of background objects. In both cases one is measuring the correlations between the galaxies and dark matter along the line of sight, which can be expressed as a convolution over the galaxy-dark matter cross-correlation power spectrum.

Galaxy-dark matter cross-correlations have been modelled in the past using either a bias model relating them to the dark matter or galaxy power spectrum [18] or using galaxies sitting at the centers of the galactic size halos [5]. In the first description assuming galaxy-dark matter cross-correlations measure bias  $b(k)P_{\text{dm}}(k)$ , which in combination with the galaxy power spectrum  $b^2(k)P_{\text{dm}}(k)$  can give both  $b(k)$  and  $P_{\text{dm}}(k)$ . Such a model is a reasonable description on large scales, but must break down on small scales where galaxies do not trace dark matter and there is no guarantee that the scale dependent bias that relates  $P_{\text{gal, dm}}(k)$  and  $P_{\text{gal}}(k)$  can be used to extract  $P_{\text{dm}}(k)$ .

Second model describes cross-correlations in terms of galaxies sitting at the centers of their halos and interprets the results in terms of the averaged halo profile [5]. There are two potential problems with this approach. First, there may be more than one galaxy inside the halo, which is specially important for large halos (figure 3). Since not all galaxies can lie at the halo center this can affect the interpretation of the cross-correlations in terms of the halo profile. Second, just as in the case of the dark matter the contribution to the power spectrum comes from a range of halo masses and one cannot model the galaxy-dark matter cross-correlation simply as a typical  $L_*$  galaxy halo profile. The strength of the correlations is determined both by the dark matter profile of the halos as well as by the halo mass function, so the slope of the correlation function that one is ultimately measuring with galaxy-galaxy lensing and foreground-background galaxy correlations need not be directly related to the dark matter profile [43]. Model developed in previous sections may be applied to the dark matter-galaxy cross-correlation power spectrum to quantify these issues in more detail.

Galaxy-dark matter cross-correlation power spectrum has halo-halo and halo Poisson terms. First term describes the correlations between galaxies and dark matter in neighbouring halos and is dominant on large scales. Second term includes the correlations between the galaxies and dark matter in the same halo and dominates on small scales. The halo-halo term is given by

$$P_{g,dm}^{hh}(k) = P_{lin}(k) \left[ \frac{\bar{\rho}}{\bar{n}} \int f(\nu) d\nu \frac{\langle N \rangle}{M} b(\nu) y[k, M(\nu)] \right] \left[ \int f(\nu) d\nu b(\nu) y[k, M(\nu)] \right]. \quad (19)$$

On large scales where this term dominates it reduces to constant bias model,  $P_{g,dm}^{hh}(k) = \langle b \rangle P_{lin}(k)$ . The Poisson term in the model where galaxies trace dark matter inside the halos except for the central galaxy sitting at its center is given by

$$P_{g,dm}^P(k) = \frac{1}{(2\pi)^3 \bar{n}} \int f(\nu) d\nu \langle N \rangle |y(k, M)|^p. \quad (20)$$

Here  $p = 2$  for  $\langle N \rangle > 1$  and  $p = 1$  for  $\langle N \rangle < 1$ .

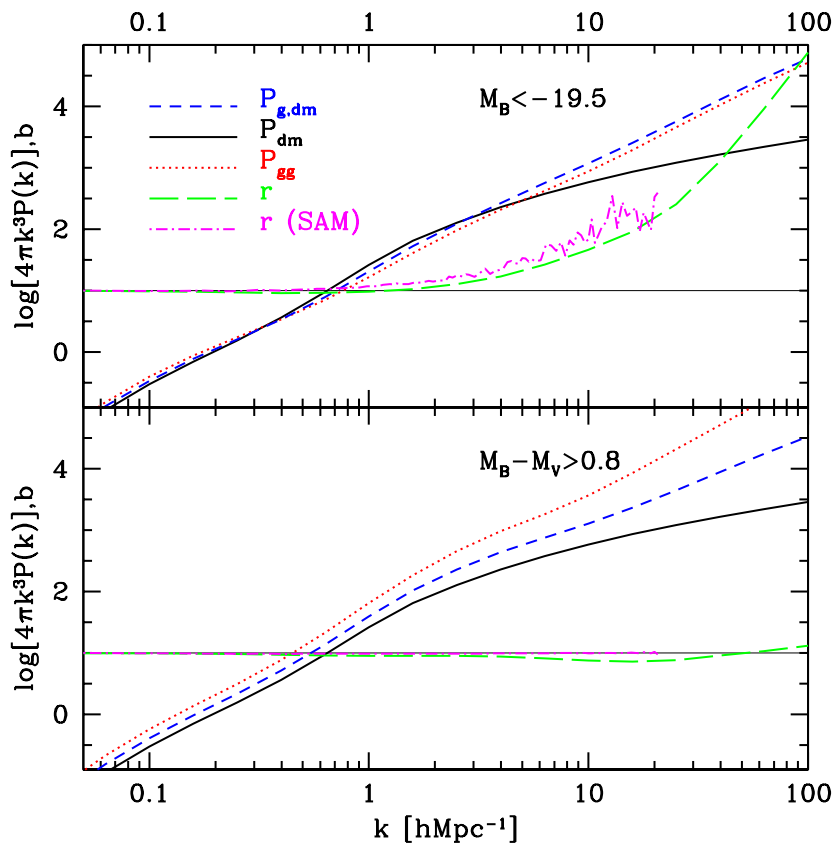


FIG. 6. Galaxy-dark matter cross-correlation power spectrum for the two galaxy types as in figure 3 (dashed), together with the dark matter (solid) and galaxy (dotted) power spectrum. Also shown is the cross-correlation coefficient  $r(k)$  from the model (dash-dotted) and from simulations (long-dashed).

Figure 6 shows the results for the cross-correlation power spectrum for the same galaxy selection as in figures 3 and 4. For regular galaxies selected by an absolute magnitude (top panel) the cross-correlation spectrum is similar to the galaxy power spectrum. If we define the cross-correlation coefficient as

$$r(k) = \frac{P_{g,dm}(k)}{[P_{dm}(k)P_g(k)]^{1/2}}, \quad (21)$$

then we see from figure 6 that it is approximately unity up to  $k \sim 1 hMpc^{-1}$  and increases for higher  $k$ . Note that the cross-correlation coefficient is not restricted to  $|r(k)| < 1$  because we have subtracted out the shot noise term from the

galaxy power spectrum following the usual approach [37]. Because on small scales the galaxy and cross-correlation spectra are comparable and exceed the dark matter spectrum the cross-correlation coefficient grows to large values in this model. Comparison with the semi-analytic results [43] again shows very good agreement up to the resolution limit of the simulations. Bottom of figure 6 shows the results for the red galaxies. In this case the cross-correlation spectrum falls in between the dark matter and the galaxy spectrum, so that  $r \sim 1$  down to very small scales. This is again in agreement with semi-analytic results which show  $r \sim 1$  throughout the entire range of  $k$ .

The main reason for  $r \neq 1$  on small scales is that  $\langle N(N-1) \rangle^{1/2} \neq \langle N \rangle$  (figure 3). The difference between the two functions is more significant for the normal than for the red galaxies, which is why the cross-correlation coefficient begins to deviate from unity at larger scales for  $M_B < -19.5$  than for  $M_B - M_V > 0.8$ . Because in this regime  $\langle N(N-1) \rangle^{1/2} < \langle N \rangle$  this leads to  $r(k) > 1$ , as seen in figure 6. It is interesting to note from figure 3 that for the red galaxies the two functions agree very well even below unity and this leads to  $r(k) \sim 1$  down to very small scales. When this happens one can reconstruct the dark matter power spectrum from the galaxy and cross-correlation spectrum even if most of the dark matter halos are not directly observed. Unfortunately one cannot extract these two functions without first identifying the dark matter halos, so this prediction cannot be directly verified from observational data using the galaxy information only.

Second source of stochasticity is the presence of central galaxy. For those halos where  $\langle N(N-1) \rangle^{1/2} < 1$  or  $\langle N \rangle < 1$  only one power of  $y(k, M)$  is used as opposed to two in the case of the dark matter. This induces some stochasticity even if  $\langle N \rangle = \langle N(N-1) \rangle^{1/2}$ , because it enhances the galaxy-galaxy and galaxy-dark matter spectrum above the dark matter-dark matter spectrum. Another source of stochasticity would be  $\psi \neq 0$ , which would make correlations at a given scale being dominated by different mass range in the case of the dark matter and the galaxies. Calculations where only this effect is present give  $r \sim 1$  over a wide range of scales, showing that this cannot be a significant source of stochasticity, at least for reasonable values of  $\psi$ .

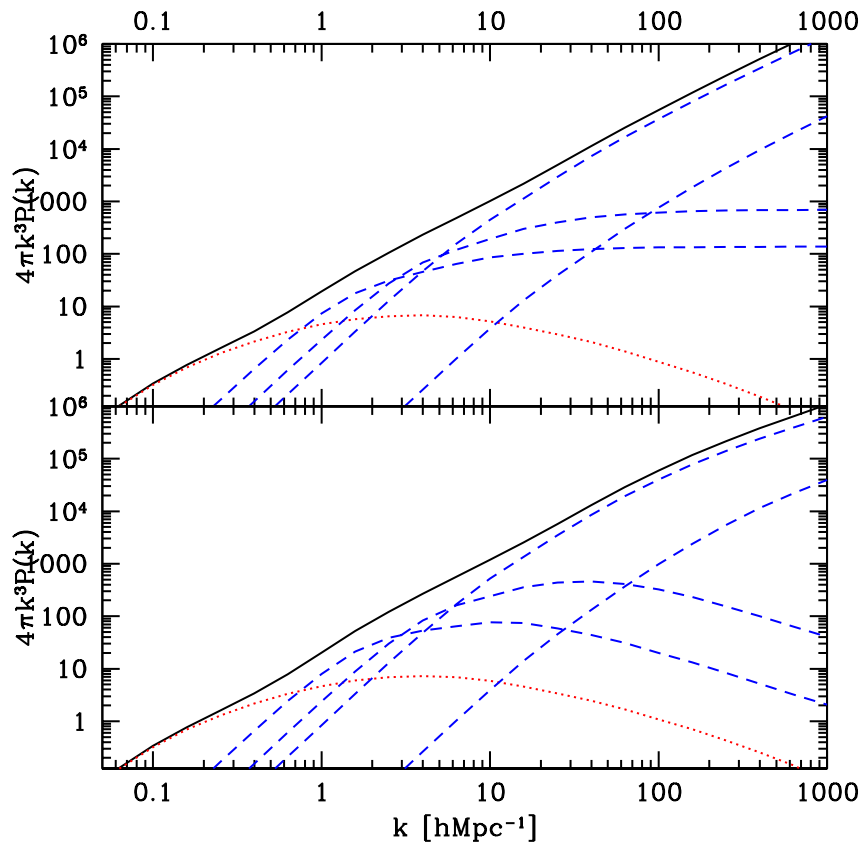


FIG. 7. Contribution to the dark matter galaxy cross-correlation power spectrum from the different halo mass intervals. The curves correspond to the same mass intervals as in figure 2. Top is  $\alpha = -1.5$  model, bottom  $\alpha = -1$ .

Our model predicts that even if the constant bias model is not valid, its generalization  $r = 1$  model may be a reasonable approximation at least down to 1 Mpc scales. An example are the red galaxies (bottom of figure 6), which have very strong scale dependent bias, yet  $r \approx 1$  over a wide range of scales. In this sense determining the

dark matter power spectrum from the measurements of galaxy-galaxy spectrum and galaxy-dark matter spectrum under the assumption of  $r = 1$  may have a larger range of validity than the constant bias model. This relies on the assumption  $\langle N \rangle = \langle N(N - 1) \rangle^{1/2}$  predicted from these models. This prediction can be verified at least for the more massive halos directly from observations, for example by using galaxy counts in cluster catalogs to extract  $\langle N \rangle$  and  $\langle N(N - 1) \rangle^{1/2}$ . Such an approach would provide an alternative way to determine  $r(k)$  directly from the data.

The model developed here can also be used to clarify the interpretation of the galaxy-dark matter cross-correlation in terms of an averaged density profile of a typical galaxy. Figure 7 shows the contribution to the cross-correlation spectrum from the different halo mass intervals, similar to figure 2 for the dark matter. For  $k < 20h\text{Mpc}^{-1}$ , corresponding approximately to scales larger than  $100h^{-1}\text{kpc}$  in real space, one cannot interpret the correlations in terms of the shape of a single halo profile, but instead as the convolution of these over the halo mass function, multiplied with the number of galaxies per halo. Observed correlations on large scales do not necessarily mean that the halo of an  $L_*$  galaxy extends to large distances. Instead, it is more likely that one is observing correlations arising from the group and cluster size halos, which exceed the correlations contributed from the galactic size halos on larger scales. This cannot be corrected in any simple manner by taking into account the correlation function of the galaxies [17], which attempts to model the presence of other nearby halos. Even if the galaxy correlations vanished one would still need to take into account the halo mass function and the fact that different halos dominate on different scales. More detailed discussion of these points will be presented elsewhere [43].

On smaller scales the transition to  $\langle N \rangle(M) < 1$  implies that  $y(k, M)$  suppression is less important because  $p = 1$ . This is further enhanced by the flattening of  $\langle N \rangle$  below  $M \sim 10^{13}h^{-1}M_\odot$  as seen in figure 3. In addition, galaxies selected on the basis of their absolute magnitude cannot exist in very small halos, so the mass function has a strong cutoff below  $10^{12}h^{-1}M_\odot$ . Thus on scales with  $k > 20h\text{Mpc}^{-1}$  the galaxy-dark matter cross-correlation may be better interpreted in terms of the average profile of  $10^{12}h^{-1}M_\odot < M < 10^{13}h^{-1}M_\odot$  halos. However, this may not be a robust prediction since the semi-analytic predictions in figure 3 are highly uncertain over this mass range. A small change in  $\langle N \rangle(M)$  may lead to a larger influence of the mass function on the power spectrum, making the correspondence between the halo profile and the power spectrum less certain. In general one should be cautious in interpreting the shape of the galaxy-dark matter correlation function in terms of an averaged dark matter profile.

## V. CONCLUSIONS

We developed an analytic model for computing the power spectrum of the dark matter, galaxies and their cross-correlation based on the Press-Schechter model. In this model all the matter in the universe is divided into virialized halos. These halos cluster and have some internal profile. The total power spectrum is the sum of the halo clustering term and the halo Poisson term, which accounts for the correlations within the halos. We assume that the halo profiles are self-similar regardless of the initial conditions, but with the mass dependent concentration parameter, as suggested by high resolution simulations [9,23,21]. The model agrees well with the results of N-body simulations for the  $\Lambda\text{CDM}$  model. We are able to find a good agreement for inner slopes  $\alpha = -1$  and  $\alpha = -1.5$ , indicating that the shape of the nonlinear power spectrum cannot by itself distinguish between the two.

The model can in principle be applied to any cosmological model, including those with a cutoff in the linear power spectrum on small scales or with some features in the power spectrum. While this will be explored in more detail in a future paper we wish to emphasize here that the mass function, which is sensitive to the linear power spectrum, has a direct effect on the nonlinear power spectrum through the halo abundance, so that not all of the information on the linear power is lost in the nonlinear regime. For example, if the linear power spectrum is cut-off on small scales and if inner profile  $\alpha > -1.5$  as suggested by the simulations then the correlation function or  $k^3P(k)$  must have a turnover on small scales. This differs from the CDM models which predict the nonlinear correlation function to continue to grow on small scales. If we wish to eliminate the halos with  $M < 10^{11}h^{-1}M_\odot$  [33] then this would suppress the power on scales below  $10\text{kpc}$  (figure 2). This effect therefore becomes significant on scales smaller than those resolved in a recent study of such truncated power spectrum models [36].

Our main conclusion regarding the galaxy power spectrum is that a simple model for the dependence of the linear and pair weighted number of galaxies inside halo as a function of the halo mass can explain most of the properties of the galaxy clustering seen in more complicated models based on the N-body simulations. A power law in the galaxy correlation function with slope 1.8 is a generic prediction of the model where the number of galaxies inside the halo increases less rapidly with mass than the halo mass itself, mean number of galaxies exceeds pair weighted average and there is a central galaxy in each halo. The decline of number of galaxies per unit mass as a function of mass is predicted by the galaxy formation models [12,13,11] and has been observed in clusters [42]. It is also required to explain the pairwise velocity dispersion results [15]. For such galaxies bias first decreases below unity, because the Poisson term is smaller for them than for dark matter. This naturally explains the later onset of nonlinearity

in galaxy power spectrum compared to the dark matter, which reconciles the discrepancy between the data and the CDM models [3]. Conversely, there is no need to invoke poorly motivated models such as double power law model [3]. On large scales bias converges to a constant for these galaxies.

Red or elliptical galaxies, which are more abundant in massive halos, show a different relation: their number inside the halos increases on average more rapidly than the halo mass. In this case bias increases with  $k$  above the turnover in the power spectrum ( $k \sim 0.01h\text{Mpc}^{-1}$ ), because their Poisson term is larger than that of dark matter. In fact, the Poisson term may be so strong that it may not be negligible compared to the halo clustering term even on very large scales and one may not converge to the constant bias model.

Galaxy-dark matter correlations can also be predicted by this model. In this case one must specify the average number of galaxies per halo as a function of halo mass. Here again our model reproduces the main features present in the N-body simulations with semi-analytic galaxy formation [43]. Galaxy-dark matter cross-correlations can be measured with galaxy-galaxy lensing or correlations between foreground and background galaxies and may provide a way to break some of the uncertainties present with the galaxy clustering. For example, we have shown that even if the constant bias may not be a good approximation, cross-correlation coefficient may nevertheless be close to unity down to Mpc scales, which would allow one to extract the dark matter power spectrum from the knowledge of the galaxy and cross-correlation spectrum on scales larger than this. The main source of stochasticity ( $r \neq 1$ ) arises from the pair weighted number of galaxies inside the halo differing from the mean number of galaxies and from the (possible) existence of central galaxies in the halos.

We have emphasized that caution must be applied when interpreting the cross-correlations such as galaxy-galaxy lensing in terms of an averaged density profile of a halo. As we have shown different halo masses dominate on different scales and the correlation function reflects this combined effect of all the halos. For example, correlations at a few hundred kpc observed by galaxy-galaxy lensing [17] are more likely to be caused by group and cluster sized halos at  $r_s$  distances than by galaxy sized halos at  $r_v$  distances. More detailed work is needed to extract the structure and extent of the dark matter halos from such observations.

Perhaps the most promising direction to explore in the future is to extract the functional dependences that parametrize our model directly from the observations. If one can determine the linear and pair weighted number of galaxies as a function of halo mass and their distribution inside the halos then one can determine the galaxy power spectrum directly within this model. Similarly if one can compare the mean number of galaxies with the pair weighted number as a function of halo mass then one can predict the galaxy-dark matter cross-correlation coefficient. This is certainly feasible for clusters, which dominate the Poisson term on large scales. Current data are sparse [42], but new surveys such as SDSS or 2dF should provide sufficient statistics to make this feasible. This approach would provide an independent estimate of the scale dependence of bias and correlation coefficient on large scales. It will also provide important constraints that would need to be satisfied by any viable galaxy formation model.

I acknowledge the support of NASA grant NAG5-8084. I thank G. Kauffmann and S. White for a detailed reading of the manuscript and for providing results of GIF N-body and semi-analytic simulations and J. Guzik for help with them. I also thank R. Sheth and R. Scoccimarro for useful conversations and help in initial stages of this project and J. Peebles and U. Pen for useful discussions.

- 
- [1] A. Dekel and J. Silk, *Astrophys. J.* **303**, 39 (1986).
  - [2] D. N. Spergel and P. J. Steinhardt, preprint astro-ph/9909386 (1999).
  - [3] see e.g. a compilation in J. A. Peacock, *Mon. Not. Roy. Astron. Soc.* **284** 885 (1997).
  - [4] a review is given in M. Bartelmann and P. Schneider, submitted to *Phys. Rep.*, preprint astro-ph/9912508 (1999).
  - [5] T. G. Brainerd, R. D. Blandford and I. Smail, *Astrophys. J.* **466** 623 (1996).
  - [6] W. H. Press and P. Schechter, *Astrophys. J.* **187**, 425 (1974).
  - [7] J. McClelland and J. Silk, *Astrophys. J.* , **217**, 331 (1977).
  - [8] R. Sheth and B. Jain, *Mon. Not. Roy. Astron. Soc.* **285**, 231 (1997).
  - [9] J. Navarro, C. Frenk and S. D. M. White, *Astrophys. J.* **462**, 563 (1996).
  - [10] Similar approach has been developed independently by R. Scoccimarro and R. Sheth (in preparation, 2000).
  - [11] M. Blanton, R. Cen, J. P. Ostriker and M. A. Strauss *Astrophys. J.* **522** 590 (1999); F. R. Pearce et al., *Astrophys. J.* **521** L99 (1999).
  - [12] A. J. Benson, S. Cole, C. S. Frenk, C. M. Baugh and C. G. Lacey, *Mon. Not. Roy. Astron. Soc.* in press, astro-ph/9903343 (1999).
  - [13] G. Kauffmann, J. M. Colberg, A. Diaferio and S. D. M. White, *Mon. Not. Roy. Astron. Soc.* **303** 529 (1999); *ibid* *Mon.*

Not. Roy. Astron. Soc.**307** 529 (1999).

- [14] see e.g. a compilation in J. A. Peacock and S. J. Dodds, Mon. Not. Roy. Astron. Soc.**267** 1020 (1994).
- [15] Y.P. Jing, H.J. Mo and G. Boerner, *Astrophys. J.* **494**, 1 (1998).
- [16] A. J. Benson, C. M. Baugh, S. Cole, C. S. Frenk and C. G. Lacey, Mon. Not. Roy. Astron. Soc.submitted, astro-ph/9910488 (1999).
- [17] I. P. Dell’Antonio and J. A. Tyson, *Astrophys. J.* bf 473, L17 (1996); M. J. Hudson, S. D. J. Dwyer, H. Dahle and N. Kaiser, *Astrophys. J.* **503** 531 (1998); R. E. Griffiths, S. Casertano, M. Im and K. U. Ratnatunga, Mon. Not. Roy. Astron. Soc.**282** 1159 (1996); Fischer et al. astro-ph/9912119 (1999).
- [18] L. van Waerbeke, *ã***334** L1 (1998).
- [19] A. Huss, B. Jain and M. Steinmetz, *Astrophys. J.* **517** 64 (1999).
- [20] G. Tormen, F. R. Bouchet and S. D. M. White, Mon. Not. Roy. Astron. Soc.**286** 865 (1997).
- [21] B. Moore, , F. Governato, T. Quinn, J. Stadel and G. Lake, *Astrophys. J.* **499** L5 (1998); B. Moore, T. Quinn, F. Governato, J. Stadel and G. Lake, astro-ph/9903164 (1999).
- [22] T. Fukushige and J. Makino, *Astrophys. J.* **477** L9 (1997).
- [23] A. V. Kravtsov et al., *Astrophys. J.* **502** 48 (1998).
- [24] Y. P. Jing and Y. Suto, *Astrophys. J.* in press, astro-ph/9909478 (1999).
- [25] J. S. Bullock, Mon. Not. Roy. Astron. Soc.submitted, astro-ph/9908159 (1999).
- [26] M. A. K. Gross et al., Mon. Not. Roy. Astron. Soc.**301**, 81 (1998); R. S. Somerville, G. Lemson, T. S. Kolatt and A. Dekel, Mon. Not. Roy. Astron. Soc., in press (astro-ph/9807277) (2000).
- [27] R. K. Sheth and G. Tormen, Mon. Not. Roy. Astron. Soc.**308**, 119 (1999).
- [28] S. Cole and N. Kaiser, Mon. Not. Roy. Astron. Soc.**237** 1127 (1989).
- [29] H. J. Mo and S. D. M. White, Mon. Not. Roy. Astron. Soc.**282**, 347 (1996).
- [30] G. Tormen, A. Diaferio and D. Syer, Mon. Not. Roy. Astron. Soc.**299**, 728 (1998).
- [31] J. A. Peacock and S. J. Dodds, Mon. Not. Roy. Astron. Soc.**280** L19 (1996).
- [32] Y. Sigad, et al., to be submitted (2000).
- [33] M. Kamionkowski and A. R. Liddle, preprint astro-ph/9911103 (1999).
- [34] D. J. Eisenstein, W. Hu, J. Silk and A. S. Szalay, *Astrophys. J.* bf 494, L1 (1998).
- [35] A. Meiksin, M. White and J. A. Peacock, Mon. Not. Roy. Astron. Soc.**304**, 851 (1999).
- [36] M. White and R. A. C. Croft, preprint astro-ph/0001247 (2000).
- [37] P. J. E. Peebles, *The Large Scale Structure of the Universe*, Princeton University Press (1980).
- [38] Jenkins, A. et al. *Astrophys. J.* **499** 20 (1998).
- [39] A. Diaferio, G. Kauffmann, J. M. Colberg and S. D. M. White, Mon. Not. Roy. Astron. Soc.**307** 537 (1999).
- [40] Y. Zeldovich, *ã***5** 84 (1970).
- [41] G. Kauffmann, A. Nusser and M. Steinmetz, Mon. Not. Roy. Astron. Soc.**286**, 795 (1997).
- [42] R. G. Carlberg et al., *Astrophys. J.* **462** 32 (1996).
- [43] J. Guzik et al., in preparation (2000).